Journal of Molecular Spectroscopy **207,** 25–31 (2001)
doi:10.1006/jmsp.2001.8303, available online at http://www.idealibrary.com on IDEAL®

The Electronic Spectrum of Germanium Monosulfide: Rotational Structure in the $A^1\Pi$–$X^1\Sigma^+$ Transition in ^{70}GeS

B. J. Shetty, Sunanda Krishnakumar, and T. K. Balasubramanian[1]

Spectroscopy Division, Modular Laboratories, Bhabha Atomic Research Centre, Trombay, Mumbai 400 085, India

Received November 7, 2000; in revised form January 5, 2001; published online April 5, 2001

The emission spectrum of the specific isotopomer ^{70}GeS was excited in a microwave (2450-MHz) discharge and the $A^1\Pi$–$X^1\Sigma^+$ transition (270–430 nm) was photographed under high resolution on a 10.6-m Ebert grating spectrograph. The rotational analysis of 43 bands led to the determination of accurate vibrational and rotational constants. Making use of these constants, the potential energy curves for the $A^1\Pi$ and $X^1\Sigma^+$ states were generated by the RKR method and Franck–Condon factors and r-centroids were computed for the bands analyzed. The present extensive high-resolution study has revealed only a few localized perturbations in the $A^1\Pi$ ($v' = 4, 5, 9$) vibronic states, which contrasts with the situation in the isovalent molecules such as GeO, SiS, and SiSe.

Key Words: germanium monosulfide; electronic spectrum; rotational analysis.

INTRODUCTION

A prominent feature in the electronic spectrum of germanium monosulfide (GeS), is the $A^1\Pi$–$X^1\Sigma^+$ transition which has been the subject of early investigations under medium resolution, both in absorption and emission (*1–3*). In recent years the molecule came to be investigated in the microwave (MW) region (*4–8*). Making use of the accurate (ground state) rotational constants derived therefrom, Magat *et al.* analyzed the rotational structure of six bands (2–1, 2–0, 3–0, 4–0, 2–10, and 3–11) of the A–X system (*9*). Subsequent to this, Le Floch and Masson (*10*) reduced all the known microwave data pertaining to the different isotopic species of GeS to molecular parameters by a nonlinear least-squares fit. Recently, the $X^1\Sigma^+$ state was further characterized by extensive semiconductor diode laser (SDL) measurements of a large number of vibration–rotation transitions involving $v \leq 7$ in the various isotopomers (*11*). The only high-resolution analysis of the $A^1\Pi$–$X^1\Sigma^+$ transition reported by Magat *et al.* (*9*) was necessarily restricted to the six bands mentioned above. As pointed out by the authors themselves, the main difficulty was posed by the congestion caused by the overlapping of the rotational structures due to the three prominent isotopomers ^{70}Ge^{32}S, ^{72}Ge^{32}S, and ^{74}Ge^{32}S. The limited analysis reported in Ref. (*9*) revealed no perturbations in the $A^1\Pi$ state. But in the isovalent molecules SiO, SiS, SiSe, SiTe, and GeO (*12–17*), the $A^1\Pi$ state is known to be perturbed to various degrees by a host of singlet and triplet states arising mainly from the $\ldots\sigma^2\pi^3\pi$ configurations.

In our laboratory, for some time now, we have been systematically studying the electronic spectra of 10-valence-electron diatomics formed by silicon with group VIA elements. In continuation of this effort we recently investigated the rotational structure of the $A^1\Pi$–$X^1\Sigma^+$ system of SiSe, wherein numerous rotational perturbations were detected in the $v = 0$–4 vibrational levels of the A-state (*15*). In fact we found the perturbations in the higher levels of the A-state to be so severe that no meaningful analysis of bands with $v \geq 5$ was possible. This prompted us to commence an exhaustive investigation of the A–X transition in the GeS molecule, which is isoelectronic with SiSe, using enriched germanium isotopes, and to compare the properties of the A-state with those of the analogous state in SiSe and other isovalent molecules. In the first phase, we could produce the spectra of the specific isotopomers ^{70}GeS and ^{74}GeS and extend the A–X system in the 380–430 nm region (*18*). Employing slightly better resolution than in the previous study (*9*), we have now carried out a comprehensive rotational analysis of 43 of the A–X bands in the specific isotopomer ^{70}GeS and, in the process, characterized the $A^1\Pi$ ($v = 0$–9) and $X^1\Sigma^+$ ($v = 0$–17) vibronic states. Though not as extensive as in the isoelectronic SiSe (*15*) or isovalent GeO (*17*) molecule, a few cases of localized perturbations in the A-state have been observed in the present studies. The details are discussed in this paper.

EXPERIMENTAL DETAILS

In GeS, the isotopic complexity arises mainly due to natural germanium which is a mixture of five isotopes with significant abundances (^{70}Ge : 20.5%, ^{72}Ge : 27.4%, ^{73}Ge : 7.8%, ^{74}Ge : 36.5%, and ^{76}Ge : 7.8%), whereas sulfur can be treated as a single isotope of ^{32}S (95%). Our main objective in the present

Supplementary data for this article are available on IDEAL (http://www.idealibrary.com) and as part of the Ohio State University Molecular Spectroscopy Archives (http://msa.lib.ohio-state.edu/jmsa_hp.htm).

[1] To whom correspondence should be addressed.

0022-2852/01 $35.00

experiments was to produce the spectrum of any preselected isotopomer by techniques that used trace amounts of enriched isotopes. The spectrum of ^{70}GeS was excited in electrodeless discharge lamps using enriched ^{70}Ge (96%) isotope, the details of which are given in our earlier paper (*18*). The high-resolution spectra were photographed in the third order of a 10.6-m Ebert spectrograph equipped with a 1200-grooves mm^{-1} grating, blazed at 1 μ. This instrument yields a reciprocal dispersion of $\sim$0.18 Å/mm in the third order. A–X being the strongest transition in GeS, exposures ranging from half an hour to eight hours were sufficient to get good quality spectra on Kodak SA1 emulsion. The rotational lines were measured against iron lines excited in a Fe–Ne hollow cathode (*19*). Their vacuum wavenumbers were obtained using a standard computer program. The relative accuracy of measurements is expected to be $\pm$0.05 cm^{-1} for the sharp and unblended rotational lines.

RESULTS AND DISCUSSION

The present method of excitation produced isotopically pure spectra, free of any impurities. The A–X transition occurs in the 270- to 430-nm region. The bands are red degraded and the structure in each band reveals a strong Q-branch, a head-forming R-branch, and a P-branch, characteristic of a $^1\Pi$–$^1\Sigma$ transition. The rotational structure is well resolved even in the vicinity of the band origin. In many bands the structure extends beyond $J = 100$. In general, the rotational lines were sharp throughout, showing no signs of diffuseness. Since we obtained an isotopically pure spectrum, the analysis was straightforward for most part. Only in the case of those bands that were overlapped by the structures of the sequence bands did we encounter some difficulties. The P, Q, and R branches were readily identified and the J-numbering assigned following standard procedures based on comparison of combination differences (*20*). The rotational analysis of 43 bands involving $v'' = 0$–17 and $v' = 0$–9 has thus been carried out. The bands taken up for analysis were so chosen that they involved common vibrational levels in the upper and/or in the lower electronic states. No combination defect was detected up to the highest J observed, thereby indicating that the Λ-doubling in the $A^1\Pi$ state is negligible. The correctness of the J-numbering was further confirmed by comparing the observed combination differences in the ground state with those calculated using the accurate rotational constants derived from the microwave and SDL measurements (*11*). The ground state of GeS, being far removed from the other electronic states (just as in the isovalent molecules), is expected to be free from perturbations. However, in the $A^1\Pi$ state a few cases of localized rotational perturbations were encountered. This aspect will be discussed in detail in a later section. The bands analyzed, along with the J_{max} observed for each band, are given in Table 1. The complete listing of the vacuum wave numbers of the rotational lines with their J assignments is available as supplementary data. The rotational structure in the 0–6 band is shown as a typical example in Fig. 1.

TABLE 1

List of Bands of $A^1\Pi$–$X^1\Sigma^+$ Transition in ^{70}GeS Rotationally Analyzed with Calculated Franck–Condon Factors and r-Centroids

Bands	J_{max}	Band Origin(cm^{-1})	FCF	r–centroid /Å
0–2	128	31638.66	0.172	2.132
0–3	128	31069.61	0.210	2.156
0–4	128	30503.83	0.193	2.180
0–5	124	29941.51	0.142	2.203
0–6	124	29382.55	0.086	2.226
0–7	115	28826.91	0.047	2.249
1–0	116	33162.66	0.088	2.065
1–1	89	32589.84	0.173	2.091
1–6	83	29758.30	0.130	2.211
1–7	112	29202.78	0.142	2.234
1–8	119	28650.52	0.112	2.257
1–9	110	28101.49	0.069	2.279
1–10	97	27556.02	0.035	2.302
2–0	122	33535.24	0.155	2.048
2–1	131	32959.35	0.129	2.075
2–4	125	31252.30	0.104	2.148
2–8	112	29023.03	0.086	2.241
2–9	119	28474.09	0.123	2.264
2–10	120	27928.57	0.113	2.287
2–11	124	27386.34	0.073	2.309
2–12	105	26847.12	0.045	2.332
3–0	130	33904.47	0.190	2.031
3–10	102	28297.22	0.065	2.271
3–11	105	27755.60	0.109	2.294
3–12	119	27216.71	0.109	2.316
3–13	112	26681.12	0.079	2.338
3–14	103	26148.96	0.046	2.361
4–0	152	34270.53	0.180	2.015
4–5	87	31425.11	0.077	2.141
4–12	101	27582.62	0.057	2.301
4–13	115	27047.11	0.101	2.323
4–14	95	26514.87	0.104	2.346
4–15	112	25985.78	0.077	2.368
5–0	132	34633.25	0.142	1.998
5–15	112	26348.76	0.097	2.353
5–16	112	25823.25	0.099	2.375
6–0	130	34992.67	0.097	1.981
6–1	105	34416.93	0.090	2.007
6–17	96	25660.58	0.096	2.382
7–0	87	35349.10	0.059	1.963
7–1	130	34772.97	0.117	1.990
8–1	112	35126.22	0.111	1.974
9–1	103	35476.29	0.085	1.957

Note. A complete list of the rotational line positions in vacuum wave numbers along with their J assignments is available as supplementary data.

After arrival at the correct J-assignments in each branch, all the rotational lines of the total of 43 bands analyzed in the present studies were subjected to a simultaneous least-squares fit of the term values in the upper and lower electronic states given by the standard expression

$$T_{ev}(J) = T_{ev} + B_v J(J+1) - D_v J^2(J+1)^2 + \cdots$$

where $T_{ev} = T_e + \omega_e(v + 1/2) - \omega_e x_e(v + 1/2)^2 + \cdots$ (with $T_e = 0$ for the ground state). With no Λ-doubling detectable in the $A^1\Pi$ state, the above term value expression proved adequate for both the states. It is worthwhile to point out here that the superior accuracy inherent in the SDL measurements

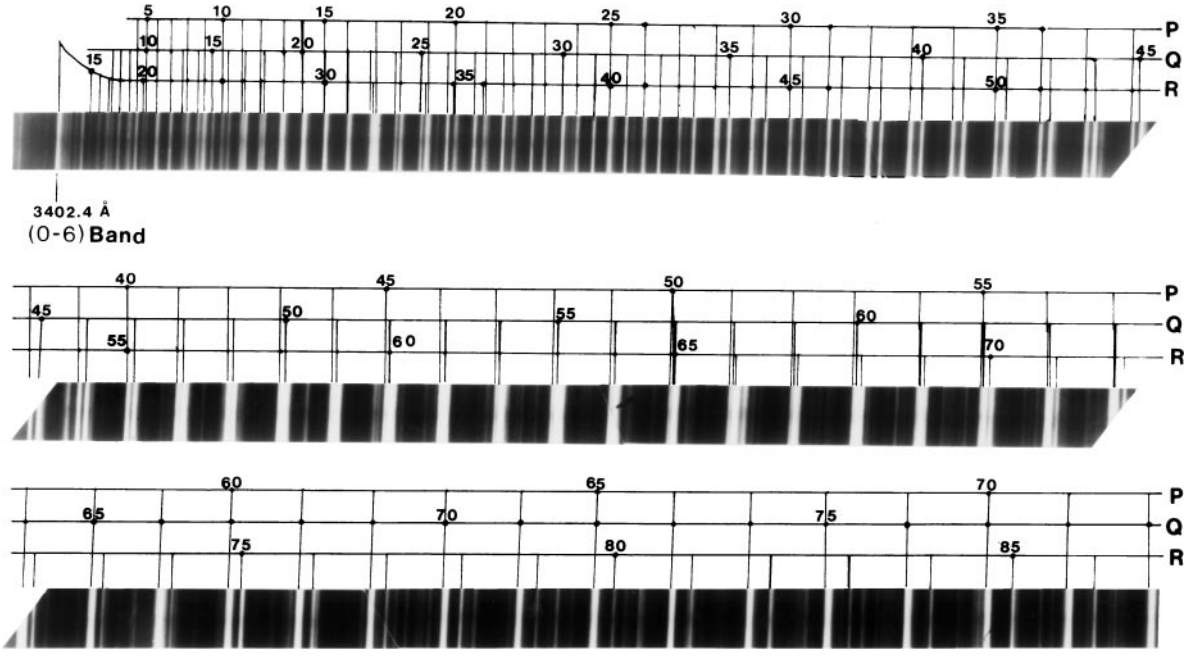

FIG. 1. Rotational structure in the 0–6 band of $A^1\Pi$–$X^1\Sigma^+$ transition in ^{70}GeS. Weaker unmarked rotational lines overlapping the main structure belong to the 2–7 band.

enabled Uehera *et al.* (*11*) to determine some of the higher order rotational constants (H_v and L_v) with statistical precision. This is not the case with the present optical spectroscopic measurements, wherein line positions are determined much less accurately. It is pertinent to point out that despite our being able to follow the branches up to $J > 120$ in some of the bands, it has not been possible to determine the higher order constants with precision. In particular, it was found that the inclusion of the higher order distortion constant H_v in the fit did not result in any improvement in the overall standard deviation. The final set of constants were obtained by fitting simultaneously all the optical (rovibronic) transitions assigned here along with the known microwave and SDL lines of ^{70}GeS through a combined least-squares procedure. To take account of the relative degrees of accuracy in the three measurements, the microwave, SDL, and present data were assigned weights of 10^8, 10^3, and 1 respectively, equal to the squares of the ratio of precision (*21*). Since no improvement of the ground state constants resulted from the above fit, the constants (B_v, D_v, H_v, and L_v) for $v'' = 0$–7 were fixed at the values determined from SDL measurements. This procedure helped us to determine the term values and rotational constants (B_v, D_v) for the other vibronic levels of the $X^1\Sigma^+$ state ($v'' = 8$–17) and $A^1\Pi$ state ($v' = 0$–9) to an accuracy that is two orders better than what would have been possible by fitting the optical data alone. The standard deviation of the fit for the present data was ± 0.04 cm^{-1} and the constants resulting from the fit are presented in Table 2. Though Magat *et al.* (*9*) had earlier carried out rotational analysis of six bands, their data could not be incorporated into our fitting procedure since they were not published. Moreover, because of the use of natural germanium in their experiments, one may not expect the quality of their data to be as good.

The vibrational term values of the two states were then separately subjected to a linear least-squares fit to determine the equilibrium vibrational constants. Since we have been able to probe higher vibrational levels, some change in the higher order anharmonicities of the ground state could be anticipated in our fit. Accordingly, the parameters ω_e'' and $\omega_e'' x_e''$ were kept fixed at the SDL values while the higher order constants $\omega_e'' y_e''$ and $\omega_e'' z_e''$ were determined by leaving them "floating." The (band-origins-based) vibrational constants for the $A^1\Pi$ state of ^{70}GeS are determined for the first time and are presented in Table 3. These are expected to be far more accurate than what was reported in our earlier work (*18*) (after appropriately transforming the values for ^{74}GeS to ^{70}GeS), deduced from vibrational analysis based on bandhead data. Also, the equilibrium rotational constants were obtained by fitting the individual B_v and D_v to polynomials in $(v + 1/2)$. Table 3 contains these results as well. For the sake of completeness, the constants determined from microwave spectroscopy (MW) and SDL data and those reported by Magat *et al.* (*9*) are included in the table. With respect to this table certain comments are in order. As far as the constants of the ground state are concerned the values derived in the present analysis are in conformity with the constants reported by Uehera *et al.* (*11*) based on SDL measurements. With respect to the upper state $A^1\Pi$, however, we were able to improve upon the constants of Magat *et al.* (*9*) and additionally provide values for many of the higher constants. This has been possible

TABLE 2
Molecular Parameters (cm^{-1}) for the $A^1\Pi$ and $X^1\Sigma^+$ States of ^{70}GeS Derived from the Rotational Analysis

v	T_v	B_v	D_v x $10^{7\dagger}$
$X^1\Sigma^+$ State:			
0	289.1800(*)	0.1894011655(*)	0.8154530510(*)
1	865.0109(*)	0.1886324786(*)	0.8162655685(*)
2	1437.4725(*)	0.1878636808(*)	0.8171017047(*)
3	2006.5677(*)	0.1870947519(*)	0.8179620974(*)
4	2572.2996(*)	0.1863256693(*)	0.8188473843(*)
5	3134.6710(*)	0.1855564083(*)	0.8197582034(*)
6	3693.6843(*)	0.1847869416(*)	0.8206951924(*)
7	4249.3420(*)	0.1840172399(*)	0.8216589891(*)
8	4801.5948(36)	0.1832608(16)	0.8314(14)
9	5350.5729(34)	0.1824880(15)	0.8328(12)
10	5896.1961(32)	0.1817152(14)	0.8332(12)
11	6438.4656(35)	0.1809394(14)	0.8290(11)
12	6977.3932(32)	0.1801770(14)	0.8380(12)
13	7512.9881(37)	0.1793976(17)	0.8324(14)
14	8045.2302(39)	0.1786288(22)	0.8365(25)
15	8574.1455(38)	0.1778552(17)	0.8391(15)
16	9099.6992(56)	0.1770865(25)	0.8385(20)
17	9621.9556(59)	0.1762893(35)	0.8188(41)
$A^1\Pi$ State:			
0	33074.8536(17)	0.1632513(06)	1.232(04)
1	33450.7101(20)	0.1622198(10)	1.233(09)
2	33823.3220(19)	0.1611804(07)	1.231(05)
3	34192.6297(24)	0.1601561(10)	1.231(07)
4	34558.7053(22)	0.1591296(07)	1.233(04)
5	34921.5277(34)	0.1581111(12)	1.235(07)
6	35281.0928(31)	0.1570696(12)	1.216(09)
7	35637.3757(31)	0.1560936(13)	1.245(09)
8	35990.4507(49)	0.1550587(24)	1.231(22)
9	36340.4051(47)	0.1540506(27)	1.238(28)

† Uehera *et al.* (*11*) have also reported the higher order rotational constants H_v and L_v. Inclusion of these higher order distortion constants in the present fit did not result in any improvement in the overall standard deviation.

* The ground state constants were fixed from SDL data.

Values in the parentheses are the standard deviations in the last two digits quoted.

largely because of the more extensive and accurate data at our disposal.

From the SDL measurements (*11*), the ground state could be characterized with respect to the levels $v'' = 0$–7. In the present study the judicious selection of bands involving $v' = 0$–9 and $v'' = 0$–17 has helped in extending this characterization for both *A* and *X* states to significantly higher vibrational levels. Making use of the presently determined molecular parameters, Franck–Condon factors and *r*-centroids were computed following standard procedure (*22*) and the results are included in Table 1. These values differ marginally from those reported earlier (*18*), the difference being due to the use of refined vibrational and rotational constants in the present calculations. The classical turning points r_{min} and r_{max} and the potential energy curves for the $A^1\Pi$ and $X^1\Sigma^+$ states generated through the RKR procedure are shown in Fig. 2.

Perturbations in the $A^1\Pi$ State

Just as in the isovalent molecules SiO, SiS, etc., the ground state of GeS derives from the configuration $(x\sigma)^2\ (w\pi)^4 \ldots X^1\Sigma^+$. This state, being far removed from the other electronic states, is expected to be free from any perturbations. The first two excited valence configurations and the states resulting therefrom are as follows:

$$\text{I} \quad (x\sigma)(w\pi)^4 v\pi \qquad {}^1\Pi, {}^3\Pi$$
$$\text{II} \quad (x\sigma)^2(w\pi)^3 v\pi \qquad {}^1\Sigma^+, {}^3\Sigma^+, {}^1\Sigma^-, {}^3\Sigma^-, {}^1\Delta, {}^3\Delta$$

In both the configurations a bonding electron is promoted to an antibonding orbital, resulting in considerable weakening of the bond. The $^1\Pi$ state resulting from configuration I is identifiable with the $A^1\Pi$ discussed in this paper, while the $^1\Sigma^+$ state deriving from configuration II is the $E^1\Sigma^+$ state known through previous investigations (*1, 3*). The $^3\Sigma^+$ and $^3\Pi$ states arising from these configurations are the upper states of the $a^3\Sigma^+$–$X^1\Sigma^+$ and

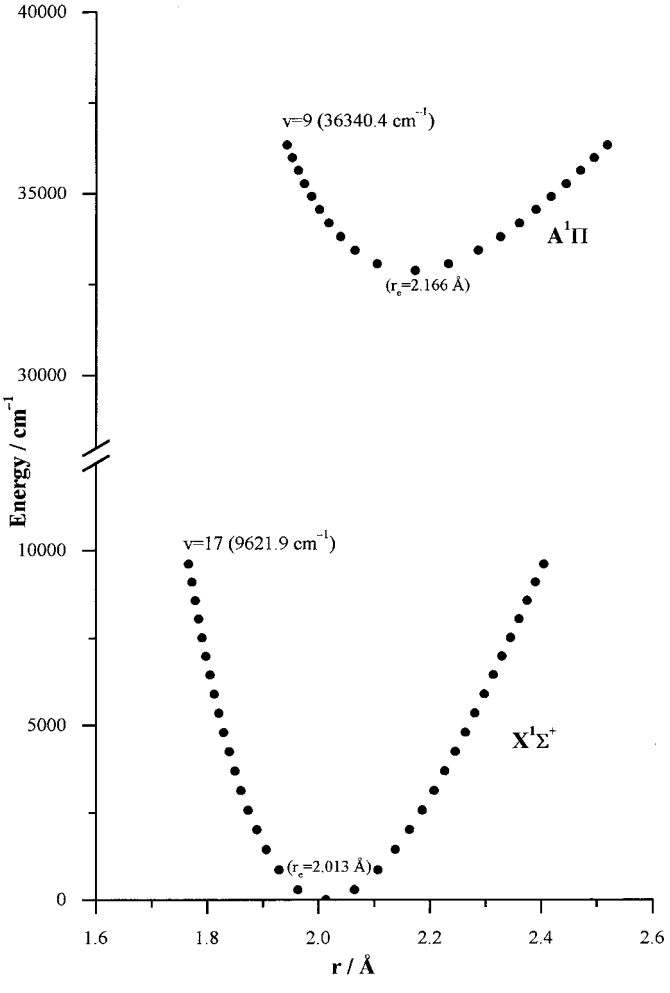

FIG. 2. Classical (RKR) turning points and potential energy curves of the $A^1\Pi$ and $X^1\Sigma^+$ states of ^{70}GeS.

TABLE 3
Molecular Constants (cm^{-1}) of the $A^1\Pi$ and $X^1\Sigma^+$ States of ^{70}GeS

	Present	Magat et al. *(9)*[a] (Reduced to ^{70}GeS)	SDL *(11)*	MW *(7)*
$X^1\Sigma^+$ State:				
ω_e	579.203478*	579.128	579.203478(309)	
$\omega_e x_e$	1.687161*	1.6593	1.687161(153)	
$10^4\,\omega_e y_e$	5.46407(4)	–16	5.563(301)	
$10^6\,\omega_e z_e$	–3.68(26)	–	–2.82(249)	
B_e[b]	0.1897854730*	–[e]	0.1897854730(636)	0.189785625
$10^4\,\alpha_e$	7.685932*	–[e]	7.685932(155)	7.68558
$10^8\,\gamma_e$	–3.95(49)	–[e]	–4.237(455)	–6.5
$10^9\,\varepsilon_e$	–3.64(72)	–	–2.599(844)	–
$10^8\,D_e$[c]	8.1505545*	–[e]	8.1505545(120)	8.3
$10^{11}\,\beta_e$	7.8951*	–	7.8951(163)	–
$10^{12}\,\delta_e$[d]	1.14(36)	–	1.1331(707)	–
$A^1\Pi$ State:				
T_e	32885.66(04)	32888.88		
ω_e	379.18(03)	378.09		
$\omega_e x_e$	1.6500(73)	1.337		
$10^3\,\omega_e y_e$	1.69(48)	–		
B_e[b]	0.163771(10)	0.16371		
$10^3\,\alpha_e$	1.0393(50)	1.01		
$10^5\,\gamma_e$	0.172(48)	–		
$10^7\,D_e$[c]	1.2313(14)	1.33		
$10^{10}\,\beta_e$	0.44(27)	–		

Values in the parentheses are the standard deviations in the last two digits quoted.
* Indicate values fixed from SDL studies.
[a] $\rho = [\mu(^{70}Ge^{32}S)/\mu(^{74}Ge^{32}S)]^{1/2} = 0.9914809$.
[b] $B_v = B_e - \alpha_e(v+1/2) + \gamma_e(v+1/2)^2 + \varepsilon_e(v+1/2)^3$.
[c] $D_v = D_e + \beta_e(v+1/2) + \delta_e(v+1/2)^2 + \xi_e(v+1/2)^3$.
[d] Uehera *et al.* (*11*) give a value $\xi_e = 1.063(790) \times 10^{-14}$ for the next higher constant.
[e] Magat *et al.* (*9*) fixed the rotational constants of the ground state ($X^1\Sigma^+$) at the microwave (*7*) values.

$b^3\Pi$–$X^1\Sigma^+$ transitions observed in chemiluminescence studies (*23, 24*). The rest of the electronic states are not involved in any direct transitions. In the isovalent molecules SiO, SiS, SiSe, SiTe, and GeO studied previously, the $A^1\Pi$ state was known to be extensively perturbed and in favorable cases the perturbing states could be characterized and accounted for by the remaining electronic states arising from configuration II (*12–17*). Therefore, it was natural to expect the situation in GeS to be similar. In fact this has been the prime motivation for us to commence the present, rather extensive investigation using an enriched isotope of germanium.

As emphasized before, until the present work of ours, the only attempt to study the A–X system of GeS under high resolution was that of Magat *et al.* (*9*), who analyzed the 2–1, 2–0, 3–0, 4–0, 2–10, and 3–11 bands. Their analysis did not reveal any perturbations in the $A^1\Pi$ state. In contrast to what is known in the other isovalent molecules, in the comprehensive study on ^{70}GeS reported here, we have observed only a limited number of localized perturbations in the $A^1\Pi$ state as summarized below:

v'	J'	e/f parity	Lines affected	Manifestation	Observed in the bands
4	53	e	$P(54)$, $R(52)$	Intensity drop	4–0, 4–5, 4–12, 4–13, 4–14, 4–15
5	29	e, f	$P(30)$, $Q(29)$, $R(28)$	Shift of levels	5–0, 5–15, 5–16
9	54	e, f	$P(55)$, $Q(54)$, $R(53)$	Shift of levels	9–1

The observed perturbations manifested either as a mere intensity drop or as a shift of the rotational lines from their expected positions. The perturbations were rather small, the observed

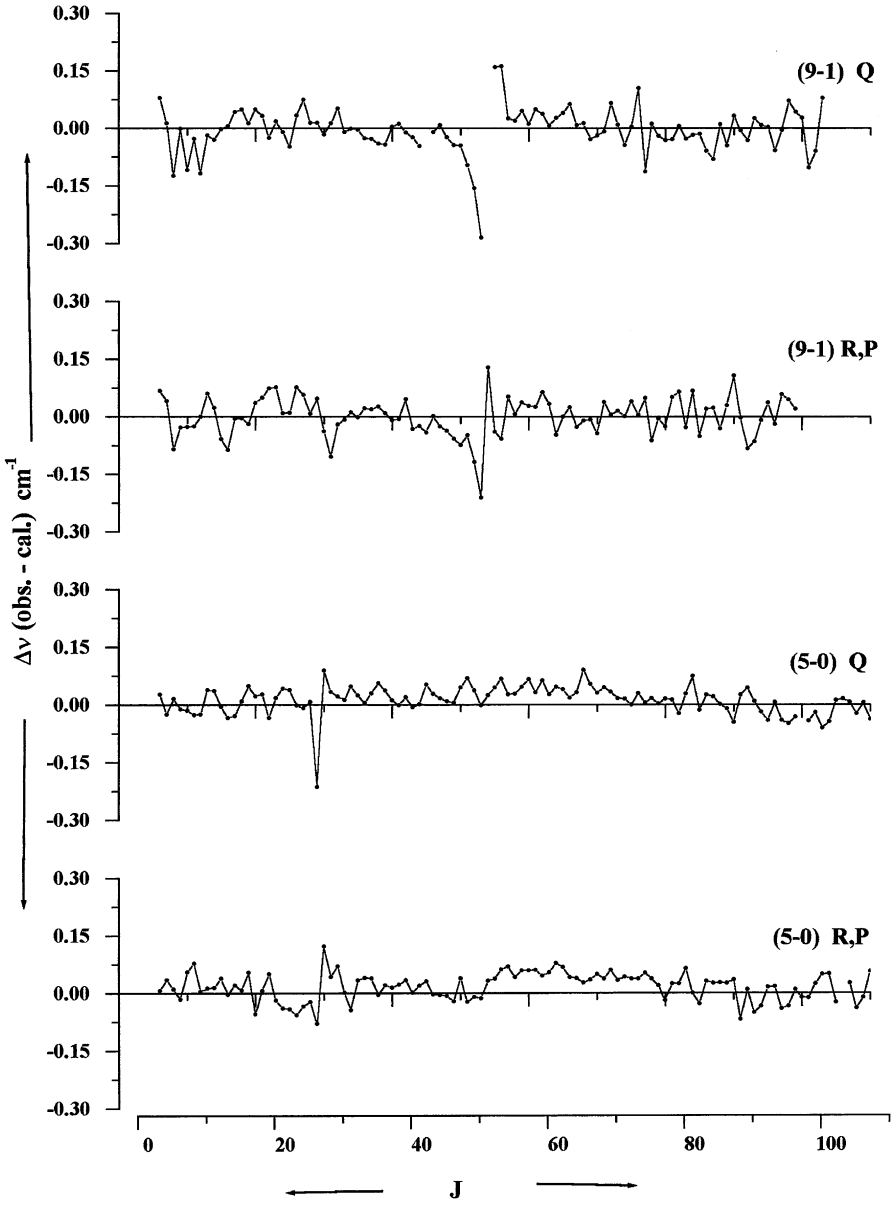

FIG. 3. Plot of $\Delta\nu$ (obs. − cal.) vs J in the bands involving $v' = 5$, 9 of the $A^1\Pi$ state, showing the observed localized perturbations.

shifts amounting not more than $\sim\pm0.2$ cm^{-1}, while the regular unblended lines could be reproduced to within ±0.04 cm^{-1}. (For lines with blends, the precision was poorer, being within ±0.1 cm^{-1}.) The observations suggestive of perturbations manifested in similar ways in bands sharing common v', which thus provided a consistency check on the inference about the perturbations. For example, the weakening of the lines $P(54)$ and $R(52)$ was common to all the bands involving the level $v' = 4$. As a typical example, Fig. 3 shows a shift in the (perturbed) rotational levels in $v' = 5$ and 9, as observed in the 5–0 and 9–1 bands. From these scanty perturbations and with no clear evidence of extra lines, it was not possible to pin down the perturbing states.

CONCLUSIONS

From the extensive high-resolution study of $A^1\Pi$–$X^1\Sigma^+$ bands of ^{70}GeS, accurate vibrational and rotational parameters for the $A^1\Pi$ state were determined. GeS showed only three localized perturbations in its $A^1\Pi$ ($v' = 4$, 5, and 9) vibronic states, in contrast to the numerous perturbations observed in its isovalent counterparts. Using the present molecular parameters, the

potential energy curves for the $A^1\Pi$ and $X^1\Sigma^+$ states were generated by the RKR method and FCFs and r-centroids were calculated for the bands analyzed.

REFERENCES

1. C. V. Shapiro, R. C. Gibbs, and A. W. Laubengayer, *Phys. Rev.* **40,** 354–365 (1932).
2. R. F. Barrow, *Proc. Phys. Soc.* **53,** 116–119 (1941).
3. G. Drummond and R. F. Barrow, *Proc. Phys. Soc. A* **65,** 277–287 (1952).
4. J. Hoeft, Z. *Naturforsch. A* **20,** 826–829 (1965).
5. J. Hoeft, F. J. Lovas, E. Tiemann, R. Tischer, and T. Torring, *Z. Naturforsch. A* **24,** 1217–1221 (1969).
6. J. Hoeft, F. J. Lovas, E. Tiemann, and T. Torring, *J. Chem. Phys.* **53,** 2736–2743 (1970).
7. F. J. Lovas and E. Tiemann, *J. Phys. Chem. Ref. Data* **3,** 712–713 (1974).
8. W. U. Steida, E. Tiemann, T. Torring, and J. Hoeft, *Z. Naturforsch. A* **31,** 374–380 (1976).
9. P. Magat, A. C. Le Floch, and J. Lebreton, *J. Phys. B* **13,** 4143–4145 (1980).
10. A. C. Le Floch and J. Masson, *J. Mol. Spectrosc.* **103,** 408–416 (1984).
11. H. Uehara, K. Horiai, Y. Ozaki and T. Konno, *J. Mol. Struct.* **352/353,** 395–405 (1989).
12. R. W. Field, A. Lagerqvist, and I. Renhorn, *Phys. Scr.* **14,** 298–319 (1976).
13. S. M. Harris, R. A. Gottscho, R. W. Field, and R. F. Barrow, *J. Mol. Spectrosc.* **91,** 35–59 (1982).
14. G. Krishnamurty, Sheila Gopal, P. Saraswathy, and G. Lakshminarayana, *Can. J. Phys.* **61,** 714–724 (1983).
15. G. Lakshminarayana and B. J. Shetty, *J. Mol. Spectrosc.* **161,** 575–577 (1993).
16. Sheila Gopal, M. Singh, and G. Lakshminarayana, *Can. J. Phys.* **70,** 291–294 (1992).
17. A. Lagerqvist and I. Renhorn, *Phys. Scr.* **25,** 241–256 (1982).
18. Sunanda Krishnakumar, B. J. Shetty, and T. K. Balasubramanian, *J. Quant. Spectrosc. Radiat. Transfer* **62,** 485–493 (1999).
19. H. M. Crosswhite, "The Iron–Neon Hollow Cathode Spectrum," *J. Res. Nat. Bur. Stand. A Phys. Chem.* **79,** 17–69 (1975).
20. G. Herzberg, "Molecular Spectra and Molecular Structure. I. Spectra of Diatomic Molecules." Van Nostrand Reinhold, New York, 1950.
21. D. L. Albritton, A. L. Schmeltekopf, and R. N. Zare, "Molecular Spectroscopy: Modern Research" (K. Narahari Rao, Ed.), Vol. II, p. 1. Academic Press, New York, 1976.
22. W. R. Jarmain and J. C. McCallum, *J. Quant. Spectrosc. Radiat. Transfer* **11,** 421–426 (1971).
23. C. Linton, *J. Mol. Spectrosc.* **79,** 90–100 (1980).
24. G. J. Green and J. L. Gole, *Chem. Phys.* **46,** 67–85 (1980).